Calculation of One-Electron Redox Potentials Revisited. Is It Possible to Calculate Accurate Potentials with Density Functional Methods?

Lindsay E. Roy, Elena Jakubikova, M. Graham Guthrie, and Enrique R. Batista*

Theoretical Division, Los Alamos National Laboratory, Los Alamos, New Mexico 87545

Received: December 24, 2008; Revised Manuscript Received: April 7, 2009

Density Functional calculations have been performed to calculate the one-electron oxidation potential for ferrocene and the redox couples for a series of small transition metal compounds of the first-, second-, and third-row elements. The solvation effects are incorporated via a self-consistent reaction field (SCRF), using the polarized continuum model (PCM). From our study of seven different density functionals combined with three different basis sets for ferrocene, we find that no density functional method can reproduce the redox trends from experiment when referencing our results to the *experimental* absolute standard hydrogen electrode (SHE) potential. In addition, including additional necessary assumptions such as solvation effects does not lead to any conclusion regarding the appropriate functional. However, we propose that if one references their transition metal compounds results to the *calculated* absolute half-cell potential of ferrocene, they can circumvent the additional assumptions necessary to predict a redox couple. Upon employing this method on several organometallic and inorganic complexes, we obtained very good correlation between calculated and experimental values ($R^2 = 0.97$), making it possible to predict trends with a high level of confidence. The hybrid functional B3LYP systematically underestimates the redox potential; however, the linear correlation between DFT and experiment is good ($R^2 = 0.96$) when including a baseline shift. This protocol is a powerful tool that allows theoretical chemists to predict the redox potential in solution of several transition metal complexes a priori and aids in the rational design of redox-active catalysts.

Introduction

Density functional theory (DFT) has proven to be a powerful tool since its inception and has provided insight into the mechanisms of several important catalytic cycles in environmental, bioinorganic, and industrial chemistry.[1,2] Many of the key chemical reactions utilizing transition metal complexes describe the loss and gain of electrons with the formation or breaking of chemical bonds. Combined with electrochemical and spectroscopic evidence of the pertinent intermediates, theoretical chemists have been able to deduce favorable thermodynamic and kinetic pathways to these cycles.[3] Also, the abilities of DFT have been pushed in hopes to not only describe these reactions, but also to facilitate the rational design of catalysts with specific properties. One such property that has garnered much attention over the past several years has been the ability of DFT to accurately predict redox potentials of transition metal complexes.[4−17] The ability to predict redox potentials a priori would be highly desirable and, with such a tool, one can imagine the design of redox-active catalyst based on a combinatorial computational approach.[18,19]

Currently, there are several protocols that exist for the theoretical prediction of the standard redox potentials in solution.[4,20] One of the more popular methods uses the Born−Haber cycle shown in Scheme 1 where the standard Gibbs free energy of redox half reaction, $\Delta G^{o,redox}_{solv}$, consists of the free energy change in the gas phase and the solvation free energies of the oxidized and reduced species. Although this method has been successful for several organic systems with continuum solvation models,[21−35] modeling transition metal complexes has proven to be less reliable. Baik and Friesner first noted that

SCHEME 1: Born−Haber Cycle

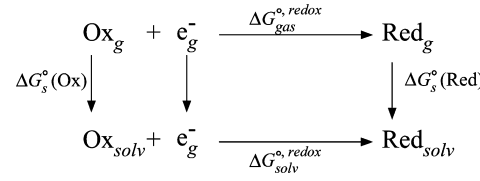

while they were able to reproduce the redox potentials of various metallocene complexes, larger deviations were seen in typical coordination complexes.[5] Uudsemaa and Tamm noted that two hydration shells and the continuum model were necessary for accurate redox calculations of aqueous 3d transition metal ions.[6] More recently, Jaque et al. showed that no DFT method can be singled out as the most reliable method for calculating the oxidation potential of Ru^{2+} in aqueous media. Srnec et al. suggest that spin−orbit coupling effects minimize the errors in the redox potential for second- and third-row transition elements.[36] In our previous work, values of the calculated redox potential for a series of small models based on the diiron hydrogenase enzymes reproduced the trends in experiment with an average error of 0.12 V using BP86 and results using B3LYP required a systematic shift.[17] This suggests that a fairly high degree of accuracy can be achieved for first-row transition elements but perhaps it might be difficult to obtain good agreement for the second- and third-row metals.

Therefore, one of the aims of this paper is to provide a theoretical treatment of ferrocene in order to assess the best basis set and functional to be used in these calculations. Ferrocene provides us a natural starting point to probe the accuracy of DFT to predict redox potentials of transition metal complexes. Aside from being recommended by IUPAC as an

* To whom correspondence should be addressed. E-mail: erb@lanl.gov.

10.1021/jp811388w CCC: $40.75
Published on Web 05/21/2009

SCHEME 2: Transition Metal Complexes Considered in This Study

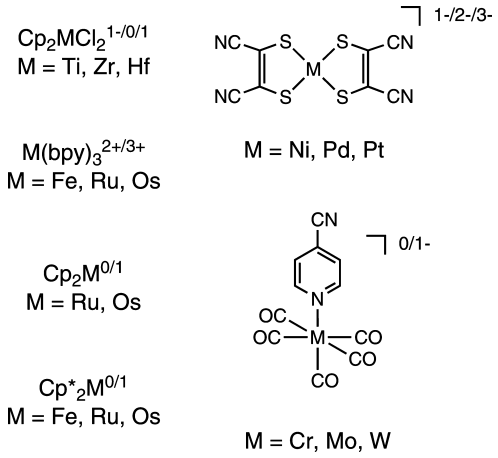

internal standard for all electrochemical experiments, the electrochemistry of ferrocene has been of interest to the experimental community for over 50 years and the $Fe^{2+}|Fe^{3+}$ couple is highly reversible and largely independent of solvent and supporting electrolyte.[37,38] From our conclusions of ferrocene, we can then move on to other transition metal complexes (shown in Scheme 2) which contain varying oxidation states and charges. These systems are comprised of first-, second-, and third-row transition elements and provide a good benchmark considering the potentials are not necessarily reversible on the electrochemical time scale.

Computational Details and Theoretical Background

Density Functional Calculations. All calculations were carried out with Gaussian 03 (Versions D.02 and E.01).[39] Geometry optimization calculations for ferrocene (Cp_2Fe) were carried out with a variety of density functional methods and basis sets. All geometries were optimized according to their respective iron basis set and functional without constraints to the lowest energy solution, the eclipsed geometry (D_{5h}), for both oxidation states. The bond distances and angles lie within the standard deviation for the functionals studied.[40] The geometries were verified by vibrational analyses at the same level of theory to ensure that they correspond to minima on the potential energy surface. All calculations were performed by using a spin-unrestricted formalism.

We examined two different DFT methods for Cp_2Fe, namely generalized gradient approximation (GGA) and hybrid-generalized gradient approximation (H-GGA). The GGA functionals considered were BLYP,[41,42] BP86,[41,43] and PBE.[44] The H-GGA used were B3LYP,[42,45] BH&HLYP,[39,41,42] B3P86,[43,45] and PBE0.[44,46,47] These functionals were chosen due to their long-standing use in computational chemistry. We tested three different basis sets for iron: LANL08,[48] which is an optimized version of the original Hay−Wadt basis set for DFT calculations, and includes an effective core potential (ECP) for the inner 10 electrons;[49] the Stuttgart RSC 1997 ECP basis set (SDD),[50] which also includes relativistic corrections to the ECP; and the all-electron basis 6-311+G*.[51] The cyclopentadienyl ion was treated with a basis set of triple-ζ quality (6-311G*) so as to be consistent with the valence basis sets used for iron. The vibrational frequencies were only scaled for BH&HLYP calculations by a factor of 0.9534 to reproduce the harmonic frequencies from experiment.[52] The frequencies derived the zero-point-energy (ZPE) and electronic, vibrational, and rotational corrections at 298.15 K for all compounds studied.

All other compounds were optimized according to their respective functional. The LANL08 basis set was used for the transition metal atoms and additional optimized diffuse and polarization functions were included for compounds containing sulfur and chlorine (LANL08d).[48,53] The 6-311G* triple-ζ with polarization basis set was used for carbon and nitrogen atoms coordinated to the metal center, and all other atoms were described by 6-31G*. The bond distances and angles for the first, second, and third row elements lie within the standard deviation for each respective functional.[40,54,55] All results in Table 5 (see below) used unscaled frequencies for the vibrational component.

Solvation Free Energies and Calculations of Redox Potentials. The solvation free energies, ΔG_s^o, for the complexes in all oxidation states were evaluated by the self-consistent reaction field (SCRF) approach based on the integral equation formalism of the polarized continuum model (IEF-PCM) level of theory, implemented as the default PCM method in Gaussian.[56] We considered two geometries using the SCRF potential: the gas-phase geometries and the complexes optimized in the presence of the reaction field. We tested several topological models to build the cavity around the complex and found that the universal force field (UFF) radii built from the UFF force field,[57] which includes individual spheres for hydrogens, produced the most accurate results for reproducing the experimental redox potential of several compounds found in Scheme 2. All SCRF calculations utilized the default options as implemented in Gaussian 03. For calculation of solvation free energies, ΔG_s^o, we used the keyword SCFVAC as implemented by Gaussian 03. The choice of solvents was based on the solvent media for all electrochemistry experiments. The dielectric constants of the solvent models were the following: dichloromethane (CH_2Cl_2), 8.93; acetone, 20.7; acetonitrile (CH_3CN), 36.64; and dimethyl sulfoxide (DMSO), 46.7. Since no solvent parameters for dimethylformamide (DMF) are implemented in Gaussian 03, we utilized the same model parameters as DMSO but incorporated a dielectric constant of 36.71, solvent radius of 2.647 Å, molar volume of 77.44 $cm^3\ mol^{-1}$, and a density of 943.87 $kg\ m^{-3}$.[58] A dielectric constant of 1.0 was used for the solute interior.

The calculated redox potentials were determined by using the free energy change of the half reactions represented by the Born−Haber cycle shown in Scheme 1[4] and consist of the free energy change in the gas phase, $\Delta G_g^{o,redox}$, and the solvation free energies of the oxidized, $\Delta G_s^o(Ox)$, and reduced, $\Delta G_s^o(Red)$, species. These values are then used to calculate the overall reaction of the standard Gibbs free energy, $\Delta G_{solv}^{o,redox}$ (in $kcal \cdot mol^{-1}$) (eq 1)

$$\Delta G_{solv}^{o,redox} = \Delta G_g^{o,redox} + \Delta G_s^o(Red) - \Delta G_s^o(Ox) \quad (1)$$

and the Nernst equation then determines the standard one-electron redox potentials, E^o (in V) (eq 2)

$$\Delta G_{solv}^{o,redox} = -FE_{calc}^o \quad (2)$$

where F is the Faraday constant, 23.06 kcal $mol^{-1}\ V^{-1}$.

The solvation free energy, ΔG_s^o, for the oxidized and reduced species is partitioned into two contributions: electrostatic and nonelectrostatic. The bulk electrostatic effects include the energy difference between the solute polarized by the reaction field of the solvent minus the nonpolarized, in vacuo solute energy. The nonelectrostatic term accounts for the sum of the cavitation and the dispersion-repulsion energies (CDR). All terms in eqs 1 and

TABLE 1: Calculated Oxidation Potential (V/SHE) for Ferrocene with the Gas-Phase-Optimized Geometry (GP-Opt) and the Reaction Field-Optimized Geometry (SCRF-Opt) in Acetonitrile (CH_3CN)[a]

	6-311+G*		LANL08		SDD	
functional	GP-Opt	SCRF-Opt	GP-Opt	SCRF-Opt	GP-Opt	SCRF-Opt
BLYP	−0.09	−0.07	−0.14	−0.15	−0.19	−0.18
BP86	0.33	0.33	0.24	0.25	0.20	0.21
PBE	0.26	0.28	0.19	0.18	0.11	0.13
B3LYP	0.60	0.59	0.67	0.67	0.65	0.66
BH&HLYP	0.62	0.62	0.68	0.69	0.66	0.67
B3P86	0.61	0.61	0.55	0.56	0.50	0.50
PBE0	0.56	0.57	0.58	0.60	0.53	0.53

[a] The experimental value is 0.65 ± 0.01 V/SHE.

TABLE 2: Calculated Oxidation Potential (V/SHE) for Ferrocene with the Gas-Phase-Optimized Geometry in Acetone and DMSO[a]

	acetone			DMSO		
functional	6-311+G*	LANL08	SDD	6-311+G*	LANL08	SDD
BLYP	0.44	0.38	0.32	0.70	0.62	0.59
BP86	0.85	0.75	0.72	1.10	1.01	0.98
PBE	0.79	0.69	0.64	1.03	0.94	0.89
B3LYP	1.10	1.18	1.16	1.42	1.42	1.41
BH&HLYP	1.14	1.22	1.18	1.39	1.46	1.44
B3P86	1.12	1.06	0.99	1.37	1.31	1.25
PBE0	1.08	1.12	1.04	1.33	1.36	1.30

[a] The experimental value is 0.72 ± 0.02 V and 0.67 ± 0.01 V/SHE for acetone and DMSO, respectively.

TABLE 3: Calculated Oxidation Potential (V/SHE) for Ferrocene in Acetonitrile (CH_3CN) with 6-31G, cc-pVTZ, and 6-311G* Basis Sets for Cyclopentadiene and LANL08 Basis Set for Fe[a]**

	6-31G**	cc-pVTZ	6-311G*
B3LYP	0.51	0.57	0.67
BH&HLYP	0.47	0.57	0.68
BP86	0.11	0.19	0.24
PBE0	0.47	0.48	0.58

[a] The experimental value is 0.65 ± 0.01 V/SHE.

2 are at 298.15 K. When considering the SCRF-optimized structure, we also included a geometry relaxation energy term, de_{geom}, to the electrostatic part of the solvation free energy. All potentials shown for ferrocene are reported versus the standard hydrogen electrode (SHE) and all others are referenced to Cp_2Fe, which is described further in the text.

Results and Discussion

DFT Calculations of the Ferrocene Oxidation Potential. To validate our method, we examined the ferrocene couple in three different solvents: acetonitrile (CH_3CN), acetone, and dimethyl sulfoxide (DMSO). Since the oxidation potential remains fairly constant across several supporting electrolytes, one would anticipate DFT to predict the same solvent trends found in experiment. Table 1 depicts the calculated oxidation potentials for ferrocene in CH_3CN with a variety of density functionals and basis sets at the optimized gas-phase and reaction field geometries; the experimental value is 0.65 ± 0.01 V vs. SHE.[37] Since our calculations are not referenced to any standard electrode, we chose to reference our results to the absolute value of the SHE in CH_3CN (−4.60 V).[59,60] The calculated oxidation potential at the optimized gas-phase geometries for ferrocene in acetone and DMSO with use of the different functionals and basis sets are given in Table 2. The experimental value is 0.72 ± 0.02 V and 0.67 ± 0.01 V vs. SHE for acetone and DMSO,[37] respectively, and our results are referenced to the absolute SHE potential in acetone (−4.13 V)[59] and DMSO (−3.83 V).[61]

The first obvious trend from the data is that the choice of basis set for iron is minor compared to the functional used in the system. We chose three different iron basis sets, all of which are commonly used in the literature and differ in their formalism, in hopes of providing a systematic study of the performance of the metal basis. Comparing the data for a given functional, the potential varies by ∼0.1 V among all of the sets studied. More importantly, the inclusion of scalar relativistic effects to the ECP in these calculations has little importance on the calculation. There appears to be more variation among the basis sets in acetone and DMSO, but the predicted values are all within the same range.

Another important consideration is the stabilization of the geometry in the continuum model where one might expect an improvement in the solvation free energies, and hence redox potentials. To the PCM model we included the additional electrostatic effect due to the structural relaxation in solution. We carried out these calculations using CH_3CN as an example and defined the structural relaxation energy as the total energy difference between reaction-field-optimized geometry and the PCM/CH_3CN single-point calculation using the in vacuo geometry. Table 1 shows that this extra correction has an effect of ∼0.01 V to the oxidation potential, hardly enough to justify its inclusion when considering a much slower convergence of the optimized structure and frequent energy oscillations. Indeed, optimization in the reaction field might prove useful for highly cationic or anionic species, but for this case the correction does not affect the results significantly.

The only variable that appears to have the greatest influence on the oxidation potential is the choice of DFT method. From the CH_3CN results, it appears that H-GGA methods better predict the experimental oxidation value than GGA methods. Of the functionals studied, the GGA functional BLYP performed the worst and underestimated the potential by ∼0.8 V; the H-GGA functionals B3LYP and PBE0 most closely reproduced the experimental value with BH&HLYP following closely behind. However, these conclusions become inverted for acetone and DMSO, and GGA functionals provide a slightly more accurate prediction for the Cp_2Fe/Cp_2Fe^+ couple. Also, there appears to be a consistent shift in oxidation potential of 0.52 (0.77) V in acetone (DMSO) versus the CH_3CN results. The H-GGA functionals all overestimate the potential by ∼0.4 V (∼0.7 V) in acetone (DMSO). While BLYP still underestimates the potential in acetone, its prediction in DMSO is better than those of its GGA counterparts. These results suggest that it is difficult to rationalize why one functional outperforms another based on the basic arguments outlining the differences in each functional method. The discrepancy seems to stem from the level of approximation evidenced by the fact that each class of functional gives similar results.

A possible source of error in our calculations could be that the ligand basis set is not appropriate and a large correlation-

TABLE 4: Calculated Oxidation Potential (V/SHE) for Ferrocene with the Gas-Phase-Optimized Geometry and LANL08 Basis Set with the Corresponding Surface Potential for CH_3CN, Acetone, and DMSO[68]

functional	CH_3CN	acetone	DMSO
BLYP	−0.24	0.07	0.38
BP86	0.14	0.45	0.77
PBE	0.09	0.39	0.70
B3LYP	0.57	0.89	1.18
BH&HLYP	0.58	0.92	1.22
B3P86	0.45	0.76	1.07
PBE0	0.48	0.82	1.12
expt	0.65	0.72	0.67

consistent basis will produce more accurate results, as suggested by Baik and Friesner.[5] In regard to ferrocene, they reported that the B3LYP/6-31G** level of theory overestimated the potential by 0.11 V whereas B3LYP/cc-pVTZ(-f)++ calculations improved the result to 0.67 V.[5,62] To a first approximation, one would not expect a great improvement using a correlation-consistent ligand basis set considering that the ferrocene couple is a solely metal-based oxidation and that these larger basis sets are usually not necessary in DFT, where they are used to expand the charge density. More importantly, one detail left out of Baik and Friesner's discussion was the modification of the metal basis set by uncontracting the exponents, and in some cases including diffuse functions, to be consistent with the triple-ζ quality basis used on the ligands. Since both metal and ligand basis sets were modified at the same time, we felt that it was important to reexamine this issue by only modifying the ligand basis set while maintaining the same Fe basis throughout. Table 3 lists the computed oxidation values for ferrocene for a selection of density functionals with 6-31G**, Dunning's correlation-consistent basis sets (cc-pVTZ),[63] and 6-311G* for the ligand basis, all with the LANL08 Fe basis set and CH_3CN as the solvent. As expected, we found improvement between the double- and triple-ζ basis sets and a systematic improvement of ∼0.10 V was observed when comparing cc-pVTZ and 6-311G*; Baik and Friesner reported the potential was lowered by 0.07 V with cc-pVTZ(-f). There are other factors that likely improved our ferrocene results compared to those of Baik and Friesner, including the PCM and topological models, but we postulate that the modified metal basis sets used throughout the paper improved their results more so than the correlation-consistent basis set for the ligands.

Our conclusions to this point are similar to those observed by Jaque et al. for the $Ru^{3+}|Ru^{2+}$ redox couple in aqueous media.[64] Even among Density Functional methods, they observed a large variation in the reduction potential. Two possible sources of error in our Born−Haber cycle (Scheme 1) include the calculated gas-phase Gibbs free energy and the solvation approximation. Considering the former, previous photoelectron spectroscopy experiments determined the adiabatic ionization potential (IP) for ferrocene is 6.72 eV.[65] Our results show the H-GGA functionals all consistently overestimate this value by ∼0.3 eV. The GGA functionals BP86 and PBE performed well with a ∼0.08 eV error whereas BLYP underestimated the IP by ∼0.4 eV. While these errors are significant, *we are also making the assumption that the free energy of solvation alone is an appropriate quantity to use when referencing a calculated redox potential to a standard reference*. The experimentally assessable quantity is the real solvation energy of ions, which consists of the chemical solvation energy and the solvent's surface potential.[61,66] The previous procedure also neglected a major part of the entropy of solvation, namely the partial loss

TABLE 5: Calculated Redox Potential (V/Cp_2Fe) for molecules in Scheme 2 with the Gas-Phase-Optimized Geometry and LANL08 Basis Set with the Corresponding Solvent

molecule	expt	B3LYP	BP86	B3P86	PBE	PBE0
		$Cp_2MCl_2^{0/1-}/CH_2Cl_2$[70]				
Ti	−1.28	−1.51	−1.40	−0.94	−1.54	−1.52
Zr	−2.09	−2.62	−2.11	−1.86	−2.20	−2.48
Hf	−2.39	−2.99	−2.38	−2.20	−2.47	−2.83
		$Cp_2MCl_2^{0/1}/CH_2Cl_2$[70]				
Ti	1.5	1.00	1.35	1.84	1.32	1.17
Zr	1.4	1.25	1.51	1.93	1.47	1.33
Hf	1.35	1.11	1.45	1.87	1.41	1.27
		$(CO)_5M(Py\text{-}CN)^{0/1-}/DMF$[71]				
Cr	−1.63	−2.50	−1.84	−1.74	−1.90	−2.42
Mo	−1.63	−2.46	−1.80	−1.69	−1.83	−2.36
W	−1.60	−2.36	−1.72	−1.59	−1.73	−2.26
		$Cp_2M^{0/1}/CH_2Cl_2$[72]				
Ru	0.56	−0.10	0.60	0.76	0.61	0.10
Os	0.36	−0.05	0.37	0.73	0.57	0.03
		$Cp^*_2M^{0/1}/CH_2Cl_2$				
Fe	−0.59[37]	−1.48	−0.56	−0.65	−0.73	−1.37
Ru	0.08[73]	−0.68	−0.11	0.08	−0.25	−0.55
Os	−0.01[73]	−0.79	−0.23	−0.04	−0.22	−0.61
		$M(bpy)_3^{2+/3+}/CH_3CN$				
Fe	0.66[37]	0.17	0.77	0.95	0.71	0.26
Ru	0.80[74]	0.46	1.05	1.23	1.01	0.57
Os	0.41[74]	0.10	0.80	0.89	0.76	0.23
		$M(mnt)_2^{2-/3-}/CH_3CN$[75]				
Ni	−2.03	−1.92	−1.66	−1.27	−1.63	−1.87
Pd	−2.26	−2.47	−1.89	−1.63	−2.07	−2.26
Pt	−2.76	−2.87	−2.08	−2.10	−2.22	−2.77
		$M(mnt)_2^{2-/1-}/CH_3CN$[75]				
Ni	−0.23	−0.62	−0.40	0.09	−0.38	−0.38
Pd	−0.05	−0.42	−0.23	0.18	−0.19	−0.40
Pt	−0.25	−0.74	−0.40	−0.04	−0.36	−0.64
rms[a]		0.54	0.24	0.37	0.22	0.44
R^2		0.96[b]	0.97	0.97[c]	0.97	0.96[d]

[a] Root mean square error. [b] Based on $y = x + 0.48$. [c] Based on $y = x - 0.28$. [d] Based on $y = x + 0.36$.

of translation on rotation entropy of solvation.[67] While our Born−Haber cycle accounts for the solvation energy, we do not consider these other solvent effects in Tables 1−3. In addition, there is also no account of the electron-transfer process occurring at the electrode surface. Omitting these effects causes significant errors when calculating the absolute potential of the SHE electrode, for example.[61,66] However, as Table 4 shows, including solvation effects still does not improve the prediction and no conclusion can still be drawn with regard to the appropriate functional.[68] These effects appear to reduce the consistent shift but the oxidation potential in acetone (DMSO) is still 0.32 (0.62) V greater than the CH_3CN results. The H-GGA functionals appear to have a smaller margin of error in the case of CH_3CN and acetone, but they still overestimate the potential in DMSO. Conversely, the GGA functionals BP86 and PBE are fairly good at predicting the potential in DMSO, but poor predictors in CH_3CN and acetone. One might expect a deviation for DMSO considering that its higher polarizability might induce more changes in the electronic distribution of the ferrocenium cation. These changes could then give rise to a larger solvation energy compared to the other solvents. Krishtalik recently examined this interaction of ferrocene in DMSO but inclusion of the intraphase potential does not change our overall conclusion.[66] While it appears that DFT methods come close, no one particular method is appropriate for correctly

predicting the oxidation couple of ferrocene versus SHE in various polar aprotic solvents. It is evident that a systematic error appears to be missing and we will show that the trends for the family of compounds of Scheme 2 are well reproduced by both types of functional.

Redox Potential Calculations for Transition Metal Complexes. The above-mentioned assumptions all appear to be solvent related and are therefore necessary whenever one is referencing a calculated redox potential to a standard reference electrode like SHE or SCE. However, it occurred to us that the surface potential and other assumptions not considered above would effectively cancel if one references their results to a *calculated* absolute half-cell potential for the ferrocene couple (i.e., $Fc + A \rightarrow Fc^+ + A^-$), for example. It is particularly advantageous to use ferrocene because one can reduce the number of errors by using a metal basis set of similar size to that of ferrocene. Also, additional assumptions necessary for intraphase potential should be negligible for aprotic solvents since the contact will be with less polar bonds.[69]

To test our theory, we examined several different molecules shown in Scheme 2 which have known redox potentials. We focused our attention on both inorganic and organometallic compounds with various charges and ligand sets. As we have seen with ferrocene, factors such as metal basis set or optimization in the reaction field are minor compared to the functional. To be consistent, we chose to continue our analysis using LANL08 and the gas-phase-optimized geometries. We can also conclude from ferrocene that BLYP is not appropriate for these studies and BH&HLYP predicts very similar results to B3LYP. Therefore, we limited our list to the GGA functionals BP86 and PBE, and the H-GGA functionals B3LYP, B3P86, and PBE0. Thus this study serves the dual purpose of (a) examining several different types of redox chemistry where the oxidation or reduction occurs at the metal or ligand and (b) evaluating our method to predict redox potentials for the first-, second-, and third-row complexes.

Results for the calculated redox potentials for the molecules in Scheme 2 are shown in Table 5. A plot of those results is illustrated in Figure 1 for B3LYP and PBE. First, the data are all consistent with one another for a given functional, regardless if the redox process occurs at the metal center or on the ligand. The errors also appear to be systematic and are not dependent on whether the compound is a first-, second-, or third-row element. The largest deviations occur around −1.5 V, which correspond to the male-nonitriledithiolate (mnt) complexes. One would expect more of an interaction between these molecules and the solvent in experiment given their high anionic charge. It is likely that the PCM model only provides a very crude estimate of the changes in the electronic distribution. Both GGA functionals provide excellent agreement with experiment and analysis of the data shows that quality of fit is 0.96 and 0.97 for BP86 and PBE, respectively. The H-GGA functionals faired the worst in terms of fit and deviation with B3LYP having the largest systematic error with an R^2 value of 0.83. In fact, B3LYP results require a consistent shift of −0.48 V for all the data (shown as a dashed line in Figure 1). When including a baseline shift for B3LYP, correlation is improved to 0.96.

From our previous section, one might have expected the H-GGA functionals to perform better when predicting the redox in CH_3CN, for example. However, we have observed similar results following this method in small models based on the diiron hydrogenase enzymes.[17] Revisiting our Born−Haber cycle, we see that the only variation occurring among each calculation is the gas-phase free-energy term, $\Delta G_g^{o,redox}$; the free energy of solvation, $\Delta\Delta G_s^o$, only

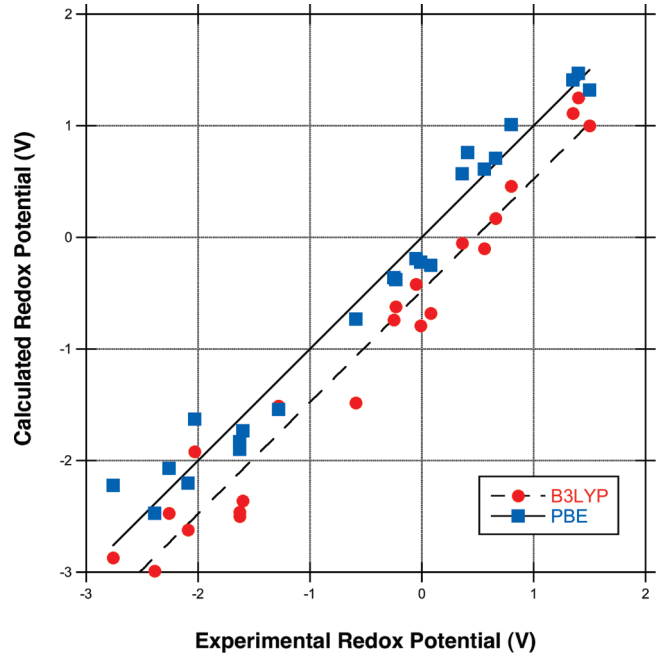

Figure 1. Correlation diagram of experimental vs. calculated redox potential, V/Cp_2Fe, for Scheme 2 complexes with B3LYP and PBE functionals. The solid line illustrates 1:1 correlation.

differs by ∼1 kcal mol^{-1} for all the functionals studied. As we have pointed out before, the GGA functionals better predict the IP for ferrocene compared to their H-GGA counterparts. Perhaps the better performance of the GGA functionals with respect to the H-GGA could be a result of an improved gas-phase IP for the molecules in Scheme 2 *and* an error cancellation of the additional solvent and/or metal electrode surface effects taking place in experiment. In light of these results, we recommend using a calculated absolute potential of a standard reference, such as ferrocene, when comparing DFT redox potentials to experiment.

Conclusion

The results outlined in this work serve as a caveat to all those calculating redox potentials of transition metal complexes using DFT. It is *not* appropriate to use the free solvation energy alone when referencing results to standard electrode such as SHE. Doing so can lead to false conclusions especially if one is predicting the redox couple of a compound a priori. To circumvent the additional assumptions necessary to predict a redox couple, one should reference all computed results to the calculated absolute half-cell potential of ferrocene for transition metal compounds. The calculated absolute value of the SHE electrode by Cramer, Truhlar, and co-workers[76] should be sufficient for organic complexes if one is using a basis set of similar size and solvation model developed by Kelly, Cramer, and Truhlar.[77,78] Of the most commonly used functionals, BP86 and PBE provide accurate results for several early-, middle-, and late-transition metal complexes and very good correlation between calculated and experimental values ($R^2 = 0.97$), making it possible to predict trends with a high level of confidence. The deviation is ∼0.16 V for the redox couple of neutral species but larger for highly anionic or cationic complexes.

Acknowledgment. This work was supported by the Laboratory Directed Research and Development (LDRD) program at Los Alamos National Laboratory. Los Alamos National Laboratory is operated by Los Alamos National Security, LLC, for the National Nuclear Security Administration of the U.S. Department of Energy under contract DE-AC52-06NA25396.

Supporting Information Available: The calculated gas-phase Gibbs free energies, free energy of solvation, and additional results on the compounds studied. This material is available free of charge via the Internet at http://pubs.acs.org.

References and Notes

(1) Maseras, F.; Lledos, A., Eds. *Computational Modeling of Homogeneous Catalysis*; Kluwer Academic Publishers: Dordrecht, The Netherlands, 2002; p 365.

(2) Rothenberg, G. *Catalysis: Concepts and Green Applications*; Wiley-VCH: Weinheim, Germany, 2008; p 279.

(3) Koch, W.; Holthausen, M. C. *A Chemist's Guide to Density Functional Theory*, 2nd ed.; Wiley-VCH: Weinheim, Germany, 2001; p 528.

(4) Li, J.; Fisher, C. L.; Chen, J. L.; Bashford, D.; Noodleman, L. *Inorg. Chem.* **1996**, *35*, 4694.

(5) Baik, M.-H.; Friesner, R. A. *J. Phys. Chem. A* **2002**, *106*, 7407.

(6) Uudsemaa, M.; Tamm, T. *J. Phys. Chem. A* **2003**, *107*, 9997.

(7) Yang, X.; Baik, M.-H. *J. Am. Chem. Soc.* **2004**, *126*, 13222.

(8) Holland, J. P.; Green, J. C.; Dilworth, J. R. *Dalton Trans.* **2006**, 783.

(9) Ayala, R.; Sprik, M. *J. Chem. Theory Comput.* **2006**, *2*, 1403.

(10) Moens, J.; Roos, G.; Jaque, P.; De Proft, F.; Geerlings, P. *Chem.—Eur. J.* **2007**, *13*, 9331.

(11) Moens, J.; Geerlings, P.; Roos, G. *Chem.—Eur. J.* **2007**, *13*, 8174.

(12) Moens, J.; Jaque, P.; De Proft, F.; Geerlings, P. *J. Phys. Chem. A* **2008**, *112*, 6023.

(13) Kuznetsov, A. M.; Maslii, A. N.; Krishtalik, L. I. *Russ. J. Electrochem.* **2008**, *44*, 34.

(14) Galstyan, A.; Knapp, E.-W. , *J. Comput. Chem.* **2008**. In press.

(15) Berard, J. J.; Schreckenbach, G.; Arnold, P. L.; Patel, D.; Love, J. B. *Inorg. Chem.* **2008**, *47*, 11583.

(16) de Groot, M. T.; Koper, M. T. M. *Phys. Chem. Chem. Phys.* **2008**, *10*, 1023.

(17) Roy, L. E.; Batista, E. R.; Hay, P. J. *Inorg. Chem.* **2008**, *47*, 9228.

(18) Endou, A.; Jung, C.; Kusagaya, T.; Kubo, M.; Selvam, P.; Miyamoto, A. *Appl. Surf. Sci.* **2004**, *223*, 159.

(19) Ito, Y.; Jung, C.; Luo, Y.; Koyama, M.; Endou, A.; Kubo, M.; Imamura, A.; Miyamoto, A. *Appl. Surf. Sci.* **2006**, *252*, 2598.

(20) Tavernelli, I.; Vuilleumier, R.; Sprik, M. *Phys. Rev. Lett.* **2002**, *88*, 213002.

(21) Reynolds, C. A. *Int. J. Quantum Chem.* **1995**, *56*, 677.

(22) Boesch, S. E.; Grafton, A. K.; Wheeler, R. A. *J. Phys. Chem.* **1996**, *100*, 10083.

(23) Raymond, K. S.; Grafton, A. K.; Wheeler, R. A. *J. Phys. Chem. B* **1997**, *101*, 623.

(24) Kaszynski, P. *J. Phys. Chem. A* **2001**, *105*, 7626.

(25) Baik, M.-H.; Schauer, C. K.; Ziegler, T. *J. Am. Chem. Soc.* **2002**, *124*, 11167.

(26) Fontanesi, C.; Benassi, R.; Giovanardi, R.; Marcaccio, M.; Paolucci, F.; Roffia, S. *J. Mol. Struct.* **2002**, *612*, 277.

(27) Namazian, M. *THEOCHEM* **2003**, *273*, 664–665.

(28) Namazian, M.; Norouzi, P.; Ranjbar, R. *THEOCHEM* **2003**, *625*, 235.

(29) Benassi, R.; Ferrarini, P.; Fontanesi, C.; Benedetti, L.; Paolucci, F. *J. Electroanal. Chem.* **2004**, *564*, 231.

(30) Namazian, M.; Almodarresieh, H. A. *THEOCHEM* **2004**, *686*, 97.

(31) Camurri, G.; Ferrarini, P.; Giovanardi, R.; Benassi, R.; Fontanesi, C. *J. Electroanal. Chem.* **2005**, *585*, 181.

(32) Dutton, A. S.; Fukuto, J. M.; Houk, K. N. *Inorg. Chem.* **2005**, *44*, 4024.

(33) Fu, Y.; Liu, L.; Yu, H.-Z.; Wang, Y.-M.; Guo, Q.-X. *J. Am. Chem. Soc.* **2005**, *127*, 7227.

(34) Shamsipur, M.; Alizadeh, K.; Arshadi, S. *THEOCHEM* **2006**, *758*, 71.

(35) Yu, A.; Liu, Y.; Li, Z.; Cheng, J.-P. *J. Phys. Chem. A* **2007**, *111*, 9978.

(36) Srnec, M.; Chalupsky, J.; Fojta, M.; Zendlova, L.; Havran, L.; Hocek, M.; Kyvala, M.; Rulisek, L. *J. Am. Chem. Soc.* **2008**, *130*, 10947.

(37) Connelly, N. G.; Geiger, W. E. *Chem. Rev.* **1996**, *96*, 877.

(38) Geiger, W. E. *Organometallics* **2007**, *26*, 5738.

(39) Frisch, M. J.; Trucks, G. W.; Schlegel, H. B.; Scuseria, G. E.; Robb, M. A.; Cheeseman, J. R.; Montgomery, J. A., Jr.; Vreven, T.; Kudin, K. N.; Burant, J. C.; Millam, J. M.; Iyengar, S. S.; Tomasi, J.; Barone, V.; Mennucci, B.; Cossi, M.; Scalmani, G.; Rega, N.; Petersson, G. A.; Nakatsuji, H.; Hada, M.; Ehara, M.; Toyota, K.; Fukuda, R.; Hasegawa, J.; Ishida, M.; Nakajima, T.; Honda, Y.; Kitao, O.; Nakai, H.; Klene, M.; Li, X.; Knox, J. E.; Hratchian, H. P.; Cross, J. B.; Bakken, V.; Adamo, C.; Jaramillo, J.; Gomperts, R.; Stratmann, R. E.; Yazyev, O.; Austin, A. J.; Cammi, R.; Pomelli, C.; Ochterski, J. W.; Ayala, P. Y.; Morokuma, K.; Voth, G. A.; Salvador, P.; Dannenberg, J. J.; Zakrzewski, V. G.; Dapprich, S.; Daniels, A. D.; Strain, M. C.; Farkas, O.; Malick, D. K.; Rabuck, A. D.; Raghavachari, K.; Foresman, J. B.; Ortiz, J. V.; Cui, Q.; Baboul, A. G.; Clifford, S.; Cioslowski, J.; Stefanov, B. B.; Liu, G.; Liashenko, A.; Piskorz, P.; Komaromi, I.; Martin, R. L.; Fox, D. J.; Keith, T.; Al-Laham, M. A.; Peng, C. Y.; Nanayakkara, A.; Challacombe, M.; Gill, P. M. W.; Johnson, B.; Chen, W.; Wong, M. W.; Gonzalez, C.; Pople, J. A. *Gaussian 03*, Revision E.01; Gaussian Inc., Wallingford, CT, 2003.

(40) Buehl, M.; Kabrede, H. *J. Chem. Theory Comput.* **2006**, *2*, 1282.

(41) Becke, A. D. *Phys. Rev. A: At., Mol., Opt. Phys.* **1988**, *38*, 3098.

(42) Lee, C.; Yang, W.; Parr, R. G. *Phys. Rev. B: Condens. Matter Mater. Phys.* **1988**, *37*, 785.

(43) Perdew, J. P. *Phys. Rev. B: Condens. Matter Mater. Phys.* **1986**, *33*, 8822.

(44) Perdew, J. P.; Burke, K.; Ernzerhof, M. *Phys. Rev. Lett.* **1996**, *77*, 3865.

(45) Becke, A. D. *J. Chem. Phys.* **1993**, *98*, 5648.

(46) Adamo, C.; Cossi, M.; Barone, V. *THEOCHEM* **1999**, *493*, 145.

(47) Ernzerhof, M.; Scuseria, G. E. *J. Chem. Phys.* **1999**, *110*, 5029.

(48) Roy, L. E.; Hay, P. J.; Martin, R. L. *J. Chem. Theory Comput.* **2008**, *4*, 1029.

(49) Hay, P. J.; Wadt, W. R. *J. Chem. Phys.* **1985**, *82*, 270.

(50) Dolg, M.; Wedig, U.; Stoll, H.; Preuss, H. *J. Chem. Phys.* **1987**, *86*, 866.

(51) Raghavachari, K.; Trucks, G. W. *J. Chem. Phys.* **1989**, *91*, 1062.

(52) Bodenheimer, J. S.; Low, W. *Spectrochim. Acta, Part A* **1973**, *29A*, 1733.

(53) Check, C. E.; Faust, T. O.; Bailey, J. M.; Wright, B. J.; Gilbert, T. M.; Sunderlin, L. S. *J. Phys. Chem. A* **2001**, *105*, 8111.

(54) Waller, M. P.; Braun, H.; Hojdis, N.; Buehl, M. *J. Chem. Theory Comput.* **2007**, *3*, 2234.

(55) Buhl, M.; Reimann, C.; Pantazis, D. A.; Bredow, T.; Neese, F. *J. Chem. Theory Comput.* **2008**, *4*, 1449.

(56) Cossi, M.; Scalmani, G.; Rega, N.; Barone, V. *J. Chem. Phys.* **2002**, *117*, 43.

(57) Rappe, A. K.; Casewit, C. J.; Colwell, K. S.; Goddard, W. A., III; Skiff, W. M. *J. Am. Chem. Soc.* **1992**, *114*, 10024.

(58) Boees, E. S.; Livotto, P. R.; Stassen, H. *Chem. Phys.* **2006**, *331*, 142.

(59) Trasatti, S. *Pure Appl. Chem.* **1986**, *58*, 955.

(60) Note that the absolute potential of SHE vary depending upon the solvent and one must use caution when referring their calculations to SHE.

(61) Fawcett, W. R. *Langmuir* **2008**, *24*, 9868.

(62) We converted their results from SCE to SHE (0.241 V) to remain consistent with our paper.

(63) Dunning, T. H. *J. Chem. Phys.* **1989**, *90*, 1007.

(64) Jaque, P.; Marenich, A. V.; Cramer, C. J.; Truhlar, D. G. *J. Phys. Chem. C* **2007**, *111*, 5783.

(65) Rabalais, J. W.; Werme, L. O.; Bergmark, T.; Karlsson, L.; Hussain, M.; Siegbahn, K. *J. Chem. Phys.* **1972**, *57*, 1185.

(66) Krishtalik, L. I.; Russ, J. *Electrochemistry* **2008**, *44*, 43.

(67) Wertz, D. H. *J. Am. Chem. Soc.* **1980**, *102*, 5316.

(68) The surface potential for CH_3CN, acetone, and DMSO is estimated to be -0.10, -0.30, and -0.24 V, respectively.[61,66]

(69) Krishtalik (ref 66) estimates this interaction in ferrocene to be ~0.1 V for CH_3CN and DMF.

(70) Loukova, G. V.; Strelets, V. V. *J. Organomet. Chem.* **2000**, *606*, 203.

(71) Kaim, W. *Inorg. Chem.* **1984**, *23*, 504.

(72) Hill, M. G.; Lamanna, W. M.; Mann, K. R. *Inorg. Chem.* **1991**, *30*, 4687.

(73) O'Hare, D.; Green, J. C.; Chadwick, T. P.; Miller, J. S. *Organometallics* **1988**, *7*, 1335.

(74) Saji, T.; Aoyagui, S. *J. Electroanal. Chem.* **1975**, *60*, 1.

(75) Geiger, W. E., Jr.; Senftleber, F. C. *J. Am. Chem. Soc.* **1975**, *97*, 5018.

(76) Kelly, C. P.; Cramer, C. J.; Truhlar, D. G. *J. Phys. Chem. B* **2007**, *111*, 408.

(77) Kelly, C. P.; Cramer, C. J.; Truhlar, D. G. *J. Chem. Theory Comput.* **2005**, *1*, 1133.

(78) As an aside, we reevaluated our ferrocene results using the calculated half-cell potential for SHE in CH_3CN and DMSO by Cramer, Truhlar, and co-workers (ref 76) and later standardized by Fawcett (ref 61) and found that the calculated oxidation potential is still off significantly. We attribute these errors to basis set and solvation model discrepancies. These results can be found in the Supporting Information.

JP811388W